Kovacs GG, Murrell JR, Horvath S, Haraszti L, Majtenyi K, Molnar MJ, et al. TARDBP variation associated with frontotemporal dementia, supranuclear gaze palsy, and chorea. Mov Disord 2009; 24: 1843–7.

Li JY, Englund E, Holton JL, Soulet D, Hagell P, Lees AJ, et al. Lewy bodies in grafted neurons in subjects with Parkinson's disease suggest host-to-graft disease propagation. Nat Med 2008; 14: 501–3.

Mackenzie IR, Baborie A, Pickering-Brown S, Du Plessis D, Jaros E, Perry RH, et al. Heterogeneity of ubiquitin pathology in frontotemporal lobar degeneration: classification and relation to clinical phenotype. Acta Neuropathol 2006a; 112: 539–49.

Mackenzie IR, Baker M, Pickering-Brown S, Hsiung GY, Lindholm C, Dwosh E, et al. The neuropathology of frontotemporal lobar degeneration caused by mutations in the progranulin gene. Brain 2006b; 129: 3081–90.

Mackenzie IR, Neumann M, Baborie A, Sampathu DM, Du Plessis D, Jaros E, et al. A harmonized classification system for FTLD-TDP pathology. Acta Neuropathol 2011; 122: 111–13.

Mahoney CJ, Beck J, Rohrer JD, Lashley T, Mok K, Shakespeare T, et al. Frontotemporal dementia with the *C9ORF72* hexanucleotide repeat expansion: clinical, neuroanatomical and neuropathological features. Brain 2012; 135: 736–50.

Murray ME, DeJesus-Hernandez M, Rutherford NJ, Baker M, Duara R, Graff-Radford NR, et al. Clinical and neuropathologic heterogeneity of c9FTD/ALS associated with hexanucleotide repeat expansion in *C9ORF72*. Acta Neuropathol 2011; 122: 673–90.

Neary D, Snowden JS, Gustafson L, Passant U, Stuss D, Black S, et al. Frontotemporal lobar degeneration: a consensus on clinical diagnostic criteria. Neurology 1998; 51: 1546–54.

Neumann M, Mackenzie IR, Cairns NJ, Boyer PJ, Markesbery WR, Smith CD, et al. TDP-43 in the ubiquitin pathology of frontotemporal dementia with *VCP* gene mutations. J Neuropathol Exp Neurol 2007; 66: 152–7.

Neumann M, Sampathu DM, Kwong LK, Truax AC, Micsenyi MC, Chou TT, et al. Ubiquitinated TDP-43 in frontotemporal lobar degeneration and amyotrophic lateral sclerosis. Science 2006; 314: 130–3.

Nonaka T, Watanabe ST, Iwatsubo T, Hasegawa M. Seeded aggregation and toxicity of α-synuclein and tau: cellular models of neurodegenerative diseases. J Biol Chem 2010; 285: 34885–98.

Renton AE, Majounie E, Waite A, Simon-Sanchez J, Rollinson S, Gibbs JR, et al. A hexanucleotide repeat expansion in *C9ORF72* is the cause of chromosome 9p21-linked ALS-FTD. Neuron 2011; 72: 257–68.

Saito Y, Kawashima A, Ruberu NN, Fujiwara H, Koyama S, Sawabe M, et al. Accumulation of phosphorylated alpha-synuclein in aging human brain. J Neuropathol Exp Neurol 2003; 62: 644–54.

Simon-Sanchez J, Dopper EG, Cohn-Hokke PE, Hukema RK, Nicolaou N, Seelaar H, et al. The clinical and pathological phenotype of *C9ORF72* hexanucleotide repeat expansions. Brain 2012; 135: 723–35.

Snowden JS, Rollinson S, Thompson JC, Harris JM, Stopford CL, Richardson AM, et al. Distinct clinical and pathological characteristics of frontotemporal dementia associated with *C9ORF72* mutations. Brain 2012; 135: 693–708.

Sreedharan J, Blair IP, Tripathi VB, Hu X, Vance C, Rogelj B, et al. TDP-43 mutations in familial and sporadic amyotrophic lateral sclerosis. Science 2008; 319: 1668–72.

Tan CF, Eguchi H, Tagawa A, Onodera O, Iwasaki T, Tsujino A, et al. TDP-43 immunoreactivity in neuronal inclusions in familial amyotrophic lateral sclerosis with or without SOD1 gene mutation. Acta Neuropathol 2007; 113: 535–42.

NEUROPATHOLOGY

Neuropathology 2012; **32**, 595–603 doi:10.1111/j.1440-1789.2012.01302.x

Original Article

Reduced brain-derived neurotrophic factor (BDNF) mRNA expression and presence of BDNF-immunoreactive granules in the spinocerebellar ataxia type 6 (SCA6) cerebellum

Makoto Takahashi,[1] Kinya Ishikawa,[1] Nozomu Sato,[1] Masato Obayashi,[1] Yusuke Niimi,[1] Taro Ishiguro,[1] Mitsunori Yamada,[4,5] Yasuko Toyoshima,[4] Hitoshi Takahashi,[4] Takeo Kato,[6] Masaki Takao,[7,*] Shigeo Murayama,[3] Osamu Mori,[8] Yoshinobu Eishi[2] and Hidehiro Mizusawa[1]

Departments of [1]Neurology and Neurological Science and [2]Pathology, Graduate School, Tokyo Medical and Dental University, [3]Department of Neuropathology (The Brain Bank for Aging Research), Tokyo Metropolitan Geriatric Hospital and Institute of Gerontology, Tokyo, [4]Department of Pathology, Pathological Neuroscience Branch, Brain Research Institute, Niigata University, [5]Department of Clinical Research, National Hospital Organization, Saigata National Hospital, Niigata, [6]Department of Neurology, Hematology, Metabolism, Endocrinology and Diabetology (DNHMED), Yamagata University Faculty of Medicine, Yamagata, [7]Department of Neurology, Institute of Brain and Blood Vessels, Mihara Memorial Hospital, Gunma, and [8]Department of Internal Medicine and Neurology, Hatsuishi Hospital, Chiba, Japan

Spinocerebellar ataxia type 6 (SCA6) is an autosomal-dominant neurodegenerative disorder caused by a small expansion of tri-nucleotide (CAG) repeat encoding polyglutamine (polyQ) in the gene for α_{1A} voltage-dependent calcium channel ($Ca_v2.1$). Thus, this disease is one of the nine neurodegenerative disorders called polyQ diseases. The Purkinje cell predominant neuronal loss is the characteristic neuropathology of SCA6, and a 75-kDa carboxy-terminal fragment (CTF) of $Ca_v2.1$ containing polyQ, which remains soluble in normal brains, becomes insoluble in the cytoplasm of SCA6 Purkinje cells. Because the suppression of the brain-derived neurotrophic factor (BDNF) expression is a potentially momentous phenomenon in many other polyQ diseases, we implemented BDNF expression analysis in SCA6 human cerebellum using quantitative RT-PCR for the *BDNF* mRNA, and by immunohistochemistry for the BDNF protein. We observed significantly reduced *BDNF* mRNA levels in SCA6 cerebellum ($n = 3$) compared to controls ($n = 6$) (Mann–Whitney *U*-test, $P = 0.0201$). On immunohistochemistry, BDNF protein was only weakly stained in control cerebellum. On the other hand, we found numerous BDNF-immunoreactive granules in dendrites of SCA6 Purkinje cells. We did not observe similar BDNF-immunoreactive granules in other polyQ diseases, such as Huntington's disease or SCA2. As we often observed that the 1C2-positive $Ca_v2.1$ aggregates existed more proximally than the BDNF-positive granules in the dendrites, we speculated that the BDNF protein trafficking in dendrites may be disturbed by $Ca_v2.1$ aggregates in SCA6 Purkinje cells. We conclude that the SCA6 pathogenic mechanism associates with the *BDNF* mRNA expression reduction and abnormal localization of BDNF protein.

Key words: brain–derived neurotrophic factor (BDNF), immunohistochemistry, Purkinje cell, quantitative reverse transcription PCR (qRT-PCR), spinocerebellar ataxia type 6 (SCA6).

Correspondence: Kinya Ishikawa, MD, PhD, Department of Neurology and Neurological Science, Graduate School, Tokyo Medical and Dental University, 1-5-45, Yushima, Bunkyo-ku, Tokyo 113-8510, Japan. Email: pico.nuro@tmd.ac.jp

*Present address: Department of Neuropathology (The Brain Bank for Aging Research), Tokyo Metropolitan Geriatric Hospital and Institute of Gerontology, 35-2, Sakaecho, Itabashi-ku, Tokyo 173-0015, Japan.

Received 22 December 2011; revised 19 January 2012 and accepted 20 January 2012; published online 7 March 2012.

INTRODUCTION

Spinocerebellar ataxia type 6 (SCA6) is an autosomal-dominant neurodegenerative disorder clinically characterized by progressive cerebellar ataxia and gaze-evoked nystagmus with an average age of onset at 45.5 years.[1,2] The disease is caused by an expansion of the tri-nucleotide (CAG) repeat encoding polyglutamine (polyQ) in the gene for the α_{1A} (P/Q-type) voltage-dependent calcium channel protein ($Ca_v2.1$).[3] Thus, SCA6 is one of the polyQ diseases which consist of nine inherited neurological disorders caused by an expansion of the polyQ tract in the causative protein. The polyQ expansion causing SCA6 exists in the cytoplasmic carboxyl(C)-tail of the $Ca_v2.1$.[3] The Purkinje cell of the cerebellar cortex, which expresses $Ca_v2.1$ most abundantly in the brain, undergoes predominant degeneration.[2,4] Although it is not clear how the polyQ expansion in $Ca_v2.1$ causes the disease, $Ca_v2.1$ aggregation specifically observed in the SCA6 Purkinje cells is likely to harbor a clue.[4,5]

SCA6 has some unique features distinct from other polyQ diseases. First, the length of the polyQ tract expansion responsible for SCA6 is remarkably short and falls within the normal range of repeats for other polyQ diseases. The lengths of CAG repeats/polyQ tract are 20–33 repeats in SCA6 patients,[6,7] while they are required to be larger than 35 repeats for being causative in other polyQ diseases such as Huntington's disease (HD).[8] Second, microscopic $Ca_v2.1$ aggregates can be seen mainly in the cytoplasm (the cell body and cell processes) of SCA6 Purkinje cells, whereas in other polyQ diseases, aggregates with expanded polyQ are prevalent in the nuclei rather than in the cytoplasm of neurons expressing the responsible proteins.[9,10] These could indicate that the pathophysiology underlying SCA6 is quite different form that of other polyQ diseases.

The brain-derived neurotrophic factor (BDNF) is a multifunctional trophic factor expressed broadly in the CNS.[11] On the other hand, the brains affected with other polyQ diseases show a reduction in the BDNF gene expression. For example, the caudate nucleus and putamen of HD brains show reduced BDNF gene expression.[12] One of the possible mechanisms underlying this reduction is the sequestration of the cyclic-AMP responsive element binding protein (CREB)-binding protein (CBP) by the expanded polyQ in the neuronal nuclei, leading to the suppression of the CREB transcription, resulting in the reduction of BDNF transcription.[13] There may be another mechanism in HD. The wild-type huntingtin activates BDNF transcription in cultured CNS neurons by a pathway independent of CREB. However, the mutated huntingtin with expanded polyQ does not activate this pathway,[14] resulting in reduced BDNF transcription. Interestingly, overexpression of the BDNF in the striatum mitigates symptoms of HD in mice,[15] suggesting that the reduction of BDNF may be a substrate for therapy of polyQ diseases.

From these backgrounds, we carried out quantitative reverse transcription PCR (qRT-PCR) analysis to assess *BDNF* mRNA expression levels, and immunohistochemistry for investigating BDNF protein localization, both to see whether expression of BDNF is also altered in SCA6 cerebellum. Given that the reduced *BDNF* mRNA expression is determined by the sequestration of CBP in affected neuronal nuclei,[16–18] SCA6 brains may not show BDNF reduction, since nuclear $Ca_v2.1$ aggregates are very few in SCA6. However, we found that *BDNF* mRNA is also suppressed in SCA6 cerebellum. Interestingly, we also found that the BDNF protein forms definable granules in the SCA6 Purkinje cell dendrites. Here, we show that BDNF expression is abnormal in SCA6 human cerebellum.

MATERIALS AND METHODS

Specimens

Brain specimens obtained at autopsy with family consent were investigated. For assessing mRNA levels by qRT-PCR, three SCA6 and six control cerebellar tissues were examined (Table 1). These six controls were from individuals without obvious neurological diseases obtained from the Research Network of Aging Brain Research, Tokyo Metropolitan Geriatric Hospital and Institute of Gerontology. For immunohistochemistry, we studied five SCA6 patients, nine controls including three HD, one for each SCA2, SCA3/Machado-Joseph disease (MJD), dentatorubral and pallidoluysian atrophy (DRPLA), one Parkinson's disease, and two SCA31 patients (Table 1). The brains were fixed in formalin, and tissue sections were embedded in paraffin. Six-micron-thick sections were used for staining.

The study was approved by the institutional review boards of ethics of Tokyo Medical and Dental University and Tokyo Metropolitan Geriatric Hospital and Institute of Gerontology, and conformed to the tenets of the Declaration of Helsinki.

RNA extraction and qRT-PCR

Human brain tissues of the cerebellar hemispheric cortices, kept frozen at –80°C after autopsy, were dissected. Total RNA was isolated from each individual by TRIzol (Invitrogen, Carlsbad, CA, USA) and RNeasy mini kit (Qiagen, Valencia, CA, USA) according to the manufacturer's protocol. Then the total RNA was treated with DNase (Invitrogen) and quantified on a nanodrop spectrophotometer (Thermo Scientific, Wilmington, DE, USA). Reverse tran-

Table 1 Profiles of the investigated patients

Diagnosis	Individual no.	Age at death (years)/gender	Repeat size	Investigations
SCA6				
SCA6	Pt. 1	75/female	13/22	qRT-PCR, IHC
SCA6	Pt. 2	76/female	13/22	qRT-PCR, IHC
SCA6	Pt. 3	66/male	15/22	qRT-PCR, IHC
SCA6	Pt. 4	79/female	13/22	IHC
SCA6	Pt. 5	68/female	13/22	IHC
Controls				
Non-neurological	Ct. 1	57/male	Not examined	qRT-PCR
Non-neurological	Ct. 2	57/male	Not examined	qRT-PCR
Non-neurological	Ct. 3	62/male	Not examined	qRT-PCR
Non-neurological	Ct. 4	62/male	Not examined	qRT-PCR
Non-neurological	Ct. 5	90/male	Not examined	qRT-PCR
Non-neurological	Ct. 6	92/male	Not examined	qRT-PCR
Huntington's disease	Ct. 7	48/female	Not examined	IHC
Huntington's disease	Ct. 8	52/male	Not examined	IHC
Huntington's disease	Ct. 9	72/female	Not examined	IHC
SCA2	Ct.10	67/male	Not examined	IHC
Machado-Joseph disease	Ct.11	65/male	Not examined	IHC
Dentatorubral & pallidoluysian atrophy	Ct.12	58/female	Not examined	IHC
Parkinson's disease	Ct.13	88/male	Not examined	IHC
SCA31	Ct.14	74/male	11/13.	IHC
SCA31	Ct.15	79/male	11/14.	IHC

IHC, immunohistochemistry; qRT-PCR, quantitative reverse-transcription polymerase chain reaction.

scription generating complementary DNA (cDNA) was carried out with random hexmers and deoxy-thymidine oligomers (oligo-dT) mixtures using a PrimeScript™ RT Master Mix (TaKaRa Bio, Tokyo, Japan). The *BDNF* and glyceraldehyde-3-phophate degydrogenase (*GAPDH*) mRNA TaqMan® Gene Expression Assays ([BDNF] = Hs00380947 = m1, [GAPDH] = 4333764T) (Applied Biosystems, Foster City, CA, USA) were purchased, and qRT-PCR was performed by LightCycler 480II (Roche, Basel, Switzerland). The *BDNF* mRNA levels were calculated against the *GAPDH* mRNA expression levels in each sample.

The *BDNF* mRNA/*GAPDH* mRNA expression ratios were calculated using the delta-delta threshold cycle (Ct) method, and were compared between controls and SCA6 group. A standard *BDNF* mRNA/*GAPDH* mRNA ratio in one control subject was expressed as 1 (standard caliber) while the rest of the samples were presented with relative values to this standard. Each experiment was repeated three times independently and was averaged (mean ± SD). Finally, the controls ($n = 6$) and SCA6 ($n = 3$) groups were compared using Mann–Whitney *U*-test.

Immunohistochemistry of human brain tissues

Immunohistochemistry was carried out as described previously.[4,5,19] For antigen retrieval, tissue blocks were boiled by exposing microwaves three times for 1 min in 10 mmol citrate buffer (pH 7.4), rinsed in distilled water and then immersed in folic acid for 5 min. Sections were incubated overnight at 4°C with one of the following three antibodies: anti-BDNF antibody (rabbit polyclonal, sc546 [alternatively named N-20],[12] diluted at 1:100 with PBS ph7.4) (Santa Cruz Biotechnology, Santa Cruz, CA, USA), 1C2 for the expanded polyQ tracts (mouse monoclonal, 5TF1-1C2, 1:4000) (Millipore, Temecula, CA, USA), and A6RPT-#5803 for $Ca_v2.1$ C-terminal region (rabbit polyclonal, 1:500).[19] The primary antibodies were serially detected with the Vectastain ABC rabbit or mouse IgG kits (Vector Laboratories, Burlingame, CA, USA), and visualized by using Histofine Simple Stain DAB (Nichirei Bioscience, Tokyo, Japan) according to the manufacturer's protocol.

For double immunofluorescent labeling, sections were similarly treated as above and incubated with primary antibodies overnight at 4°C with anti-BDNF antibody (rabbit polyclonal, 1:50) (Santa Cruz Biotechnology) and 1C2 antibody (mouse monoclonal, 5TF1-1C2, 1:2000; Millipore). Sections were washed three times in PBS and incubated with fluoresecein-labeled anti-mouse IgG (heavy and light chains [H + L]) (1:250) (Vector Laboratories) and Alexa-fluor 555 goat anti-rabbit IgG (H + L) (1:250) (Invitorogen) for 1 h at room temperature. Sections were washed three times in PBS, incubated with 1% Sudan black B in 70% methanol for 5 min to reduce the autofluorescence, washed three times in PBS and incubated with 3% 4′,6-diamidino-2-phenylindole solution for 15 min at 37°C. Slides were observed under a confocal microscope (LSM 510META; Carl Zeiss, Jena, Germany).

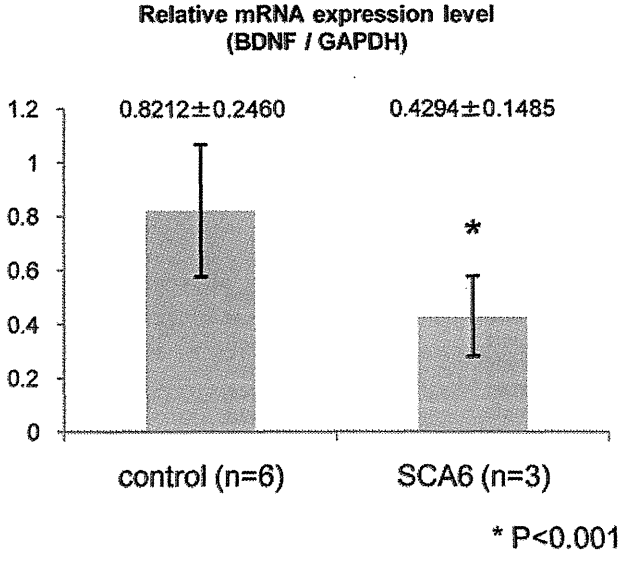

Fig. 1 Brain-derived neurotrophic factor (BDNF) expression level in spinocerebellar ataxia type 6 (SCA6) patients' cerebella is decreased in comparison with that in control patients' cerebella. Quantitative (q) RT-PCR reveals that the level of BDNF mRNA against that of glyceraldehyde 3-phosphate dehydrogenase (GAPDH) is significantly reduced in SCA6 cerebellum ($n = 3$) in comparison with controls ($n = 6$). (Control, ($n = 6$: 0.8212 ± 0.2460; SCA6, $n = 3$: 0.4294 ± 0.1485; $P = 0.0201$).

RESULTS

The *BDNF* mRNA expression level is decreased in SCA6 human cerebellum

The qRT-PCR analysis on each cDNA generated from SCA6 ($n = 3$) and control ($n = 6$) cerebellar tissues revealed that the level of *BDNF* mRNA against that of *GAPDH* mRNA was significantly reduced in SCA6 human cerebellum compared to controls (controls $n = 6$: 0.8212 ± 0.2460; SCA6, $n = 3$: 0.4294 ± 0.1485; $P = 0.0201$) (Fig. 1). This suggests that the *BDNF* mRNA expression level is decreased in SCA6 cerebellar cortex.

Observation of BDNF-immunoreactive granules in the dendrites of SCA6 Purkinje cells

To investigate whether there is a change for quantity and intracellular localization of BDNF protein in the SCA6 cerebellum, we undertook immunohistochemical analysis of SCA6 and control human cerebella with the anti-BDNF antibody. In control cerebellum, the BDNF-immunoreactivity was only weakly seen in all neurons, including the Purkinje cells and granule cells (Fig. 2a,b). The BDNF immunoreactivity was also quiescent in the SCA2 cerebellum (Fig. 2c), whereas 1C2-positive polyQ aggregates are seen in the Purkinje cell cytoplasm (Fig. 2d). In contrast, numerous BDNF-immunopositive granules were seen in the structures compatible with dendritic trees of SCA6 Purkinje cells (Fig. 2e,f, arrows). The BDNF granules were not conspicuous in the cell bodies (Fig. 2f, arrowhead) or axons of Purkinje cells. The antibody A6RPT-#5803 against the $Ca_v2.1$ C-terminus detected numerous $Ca_v2.1$ aggregates in the proximal dendrite (Fig. 2g, filled arrow) as well as in the cell body. Occasionally, they were present even in the distal part of the dendrites (Fig. 2g, open arrow), showing that the $Ca_v2.1$ aggregates exist in a wide range of dendritic arbors. The BDNF-positive structures similar to the ones seen in SCA6 Purkinje cells were sought in other areas of brains affected with polyQ diseases. However, we did not see any similar structures in as far as we investigated the cerebral cortex and the striatum of HD brains (Fig. 2h) and the pons of MJD patients. The present observation indicates that formation of BDNF-positive granules may be specific to SCA6 Purkinje cell dendrites.

BDNF-immunoreactive granules are observed in the vicinity of $Ca_v2.1$ aggregates

We next asked whether the presence of BDNF-immunoreactive granules is related to the formation of $Ca_v2.1$ aggregates known to be specific to SCA6 cell bodies and dendrites.[4,5,19] To address this question, we carried out a double immunofluorescence study against BDNF (red) and 1C2 (green).

We found that 1C2-positive polyQ aggregates often existed in the proximal portion of dendrites, such as the primary shaft (Fig. 3a, arrow) or the secondary shaft (Fig. 3b, arrow), of the Purkinje cells. On the other hand, the BDNF-immunoreactive structures were seen distal to the 1C2-positive polyQ aggregates (Fig. 3a,b). Curiously, we found that the BDNF-immunoreactive granules were seen not only within the contour of Purkinje cell dendrites (Fig. 3a,b), but also outside of the visible dendritic structures (Fig. 3c,d, arrowheads).

DISCUSSION

We made two fundamental observations in this study. One is the reduced *BDNF* mRNA level in the SCA6 cerebellum. The BDNF is a member of the neurotrophic family controlling many processes, including neurogenesis, proliferation, survival, synaptic transmission and activity-dependent synaptic plasticity.[11,13] The molecule is widely distributed in the CNS and is abundantly expressed in the cerebellar cortex, including Purkinje cells.[20] The BDNF appears to be involved in many polyQ diseases. In HD, reduced BDNF gene expression has been found in cultured cells,[14] an animal model,[15] and in patients' brains.[12,21] In addition, over-expression of BDNF gene in the striatum of

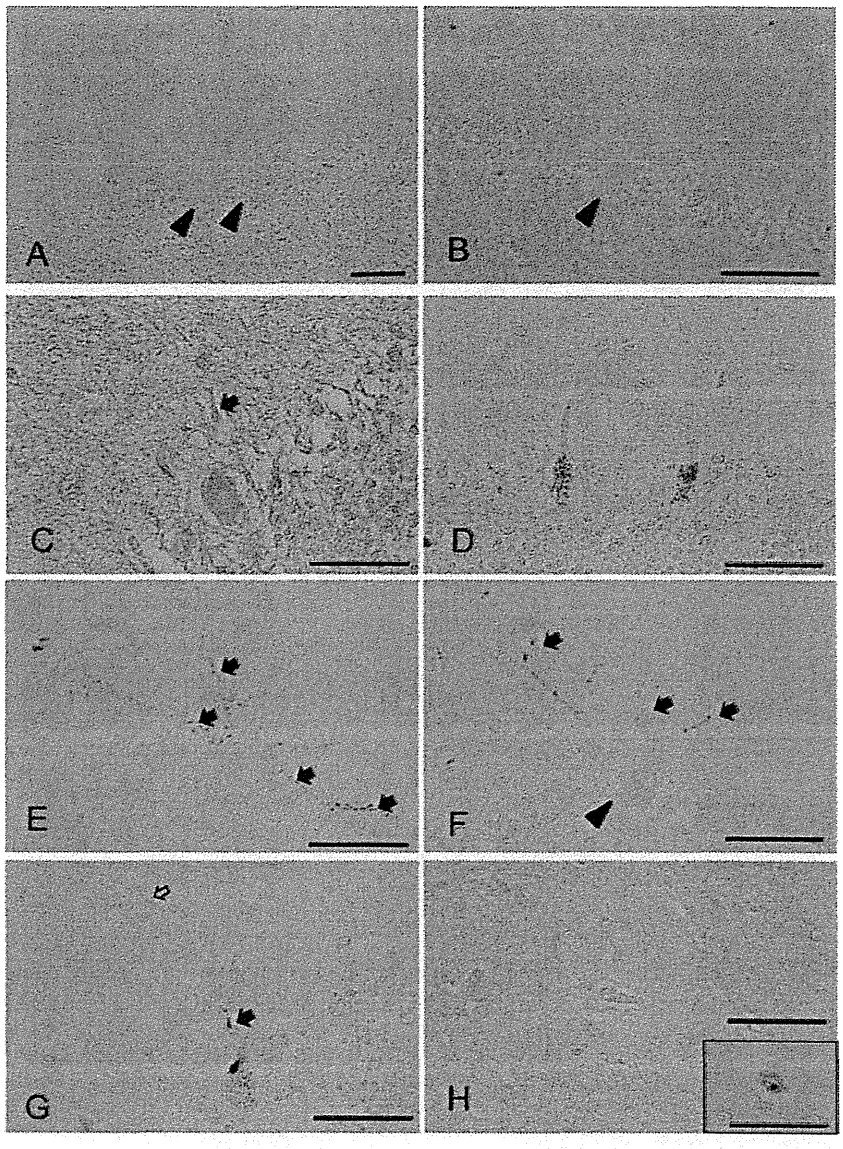

Fig. 2 Numerous brain-derived neurotrophic factor (BDNF)-immunoreactive granules are present in the dendrites of spinocerebellar ataxia type 6 (SCA6) Purkinje cells. (A, B) In control patients' cerebella, BDNF immunoreactivity is undetectable. Arrowheads indicate cell bodies of the Purkinje cells. (A, Parkinson's disease; B, SCA31). (C, D) In SCA2 cerebellum, BDNF immunoreactivity is also quiescent (C), but 1C2-positive granules are abundant in the Purkinje cell cytoplasm (D). (E, F) In a SCA6 Purkinje cell, numerous BDNF-immunoreactive granules are seen in the structures compatible with dendritic trees of Purkinje cells (arrows). BDNF granules are not conspicuous in the cell cytoplasm of Purkinje cells (arrowhead). (G) A6RPT-#5803 antibody, which is against α1A voltage-dependent calcium channel protein ($Ca_v2.1$) C-terminus, detects numerous $Ca_v2.1$ aggregates in the cell body of Purkinje cells and often in the proximal dendrite (filled arrow). $Ca_v2.1$ aggregates occasionally present even in the distal part of the dendrite (open arrow). (H) BDNF immunoreactivity is not seen in the striatum of Huntington's disease brains (large box), otherwise 1C2-positive aggregate are seen in the nuclei of striatal neurons (small box). (For A–G: scale bars; 50 μm).

HD mice compensates for reduced BDNF gene levels, ameliorating disease phenotypes.[15] The reduced BDNF gene expressions are also observed in a DRPLA cell model expressing mutant atrophin-1 and in SCA1 mouse models.[22,23] Interestingly, the drug 3,4-diaminopyridine improved motor behavior of mice by increasing BDNF expression levels.[23] These lines of evidence seem to indicate that BDNF has an important defence role in many polyQ diseases. The BDNF gene expression was also found to be reduced in affected areas of subjects with Alzheimer's disease[24] and Parkinson's disease,[25] suggesting that *BDNF* mRNA could be reduced in many neurodegenerative diseases. Considering that the BDNF is also abundantly expressed in Purkinje cells, it is possible to speculate that reduced BDNF gene expression in SCA6 cerebella may be related to the pathogenic mechanism of SCA6. However, the precise mechanism of BDNF mRNA reduction in SCA6 is not clear. While the presence of nuclear polyQ aggregates is causally associated with BDNF suppression in other polyQ diseases, such aggregates are extremely rare in SCA6 Purkinje cells.[5,19] Therefore, the mechanism reducing the BDNF gene expression in SCA6 may be different from other polyQ diseases. In cultured cell models, we recently found that the "cytoplasmic" $Ca_v2.1$ aggregates caused the reduction of CREB and phosphorylated(p)-CREB, the active CREB isoform, in the nuclei by sequestering them to the $Ca_v2.1$ aggregates in the cytoplasm (manuscript submitted). In SCA6 human brains, we also confirmed that CREB also co-localizes with $Ca_v2.1$ aggregates in Purkinje cell bodies. Thus, we speculate that the

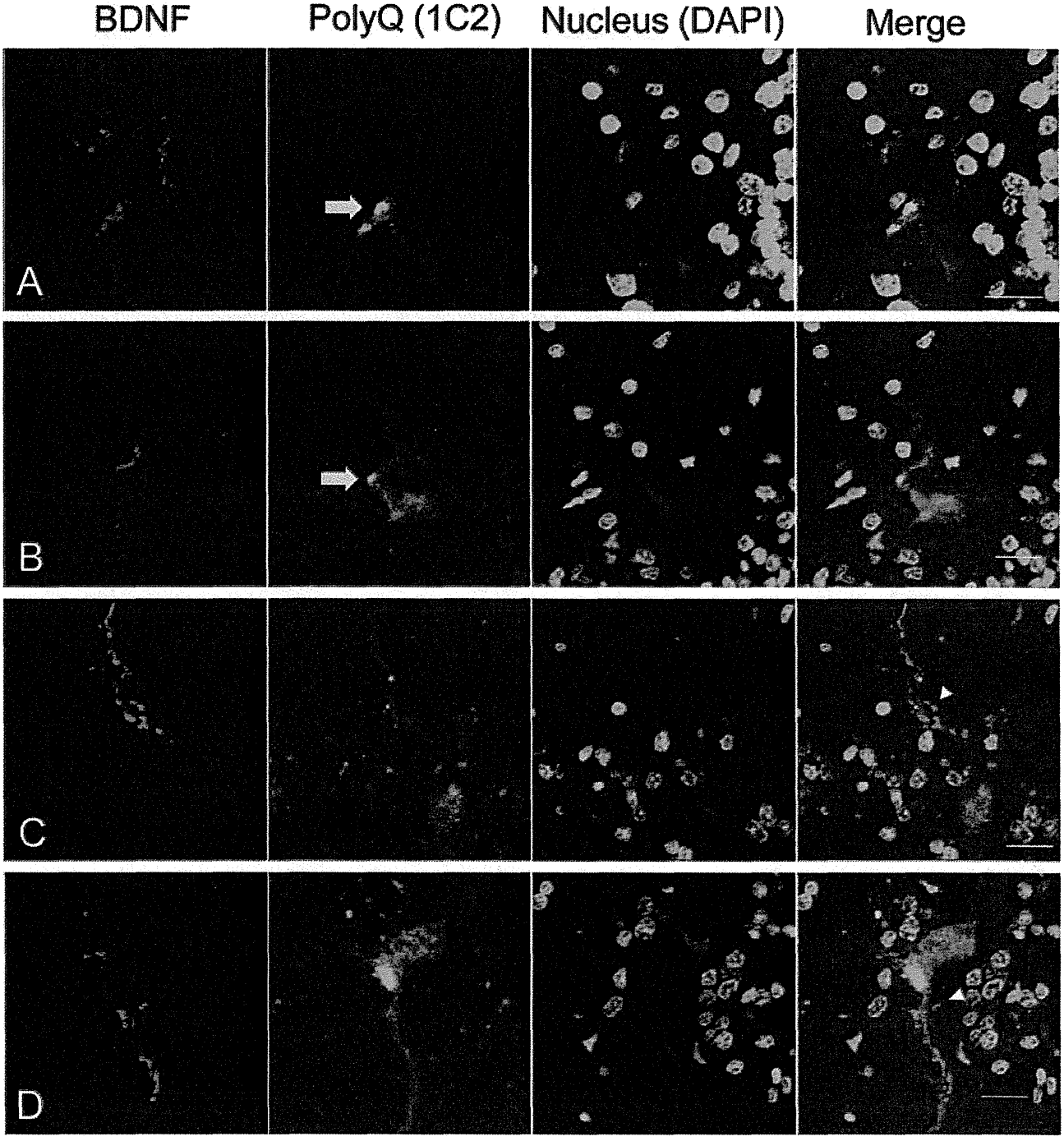

Fig. 3 The brain-derived neurotrophic factor (BDNF)-immunoreactive granules are observed in the vicinity of α1A voltage-dependent calcium channel protein (Ca,2.1) aggregates. Double immunofluorescence with 1C2 antibody and anti-BDNF antibody in spinocerebellar ataxia type 6 (SCA6) patient cerebella. (A, B) 1C2-positive polyglutamine (polyQ) aggregates often existed in the proximal portion of dendrites, such as the primary shaft (A; arrow) or the secondary shaft (B; arrow), of Purkinje cells. BDNF-immunoreactive structures were seen distal to the 1C2-positive polyQ aggregates (A, B). (C, D) BDNF-immunoreactive granules were seen not only within the contour of Purkinje cell dendrites, but also outside the visible dendritic structures (arrow head). (For A–D: scale bars: 20 μm).

reduction of BDNF gene expression is due to reduced amounts of CREB in the nuclei by sequestration of CREB in the cytoplasm by $Ca_v2.1$ aggregates. Further studies are needed to elucidate how the cytoplasmic aggregates cause the suppression of CREB-target transcription.

The other key finding in the present study is that there are abundant BDNF-immunoreactive granules, mainly in the dendrites of SCA6 Purkinje cells. Previous studies indicate that these BDNF-immunoreactive granules are not stained by ubiquitin antibodies, since SCA6 lacks ubiquitin-positive structures.[4,26] As far as we have investigated in five SCA6 cerebellar specimens, the BDNF-immunoreactive granules were restricted to the Purkinje cells, similar to the $Ca_v2.1$ aggregates. For example, we did not observe any BDNF aggregates in the cerebellar granule cells or in the neurons of the dentate nucleus. Further studies using larger numbers of SCA6 patients would be important to address whether the BDNF granules are also seen in other SCA6 brain regions. Although we observed many BDNF-immunoreactive granules within dendrites under light microscopy, we also suspected that some of these granules appear to exist outside the dendritic contour. It may be possible that they are still inside the small dendritic sprouts, which were only invisible due to degeneration. Alternatively, they may have been secreted from the dendrites as previously postulated.[27] Precise investigation using electron microscopes is needed.

Previous studies investigating the BDNF immunohistochemistry in adult rat, guinea pig and Japanese macaque cerebella have shown that BDNF is expressed diffusely in the cell body and the dendrites of Purkinje cells.[20,28,29] One previous study describes granular BDNF immunoreactivity in the control human Purkinje cell dendrites, although detailed information is not available.[30] In the present study, we observed that BDNF immunoreactivity was very weak in human post mortem control specimens. This discrepancy in the immunostaining intensities between previous studies and the present one may be due to differences in tissue preparation, such as fixation: paraformaldehyde[12] or paraformaldehyde with picric acid[26] may be more suitable fixations for BDNF immunohistochemistry than the formalin we employed. Nevertheless, the granular BDNF-immunoreactive granules in Purkinje cells were specific to SCA6 in the present cohort, indicating that this finding is meaningful.

It is remains unclear how BDNF-immunoractive granules are formed in SCA6 Purkinje cells. The BDNF protein, still translated from reduced BDNF mRNA, needs to be subjected to many processes, such as post-translational modification and needs to be transported in cells to become functional. As we observed 1C2-immunoreactive $Ca_v2.1$ aggregates in the proximal portion of the dendrites, such as the primary shaft, it is tempting to speculate that BDNF trafficking in the dendrites may be disturbed, resulting in the formation of visible BDNF-immunoreactive granules in dendrites of SCA6 Purkinje cells. The $Ca_v2.1$ aggregates, shown by A6RPT-#5803 immunohistochemistry (Fig. 2g), were seen in the cell body through distal dendrites, suggesting that the $Ca_v2.1$ aggregates widely prevail in the somato-dendritic cytoplasm. The BDNF normally moves in the dendrites in both directions (antero- and retro-grade transports) between the post-synaptic button and cell body,[31] as well as from the cell body to the presynaptic terminal through anterograde axonal transport. Therefore, it may be possible that $Ca_v2.1$ aggregates disturbed BDNF trafficking in the dendrites. Interestingly, SCA2, which also forms polyQ aggregates in the cytoplasm of Purkinje cells (Fig. 2c), did not show similar BDNF-immunoreactive granules in the dendrites of Purkinje cells. Therefore, it may be possible that a certain factor specific to $Ca_v2.1$ may underlie formation of BDNF-positive granules. For example, the secretion of BDNF from dendrites (post-synaptic secretion) is considered regulated by intracellular Ca^{2+} concentration, which is in turn regulated by *N*-methyl-D-aspartate receptors, inositol tri-phosphate receptor (IP3R) and voltage-dependent calcium channels including $Ca_v2.1$.[32] Further studies are needed to address how $Ca_v2.1$ formation leads to BDNF-immunoreactive granules in the dendrites.

In conclusion, the decrease of BDNF gene expression level and abnormal BDNF-immunoreactive granules were seen in SCA6 cerebellum. Precise understanding of the implication of altered gene expressions, including BDNF, and of the mechanism generating BDNF-immunoreactive granules, may be important for establishing fundamental therapies for SCA6.

ACKNOWLEDGMENTS

This study was funded by the Japanese Ministry of Education, Sports and Culture (KI and HM), the Japan Society for Promotion of Science (JSPS) (KI and HM), the 21st Century COE Program on Brain Integration and its Disorders from the Japanese Ministry of Education, Science and Culture (HM), the Strategic Research Program for Brain Sciences by the Ministry of Education, Culture, Sports, Science and Technology of Japan (HM), Core Research for Evolutional Science and Technology (CREST), Japan Science and Technology Agency (JST), Saitama, Japan (HM), from the Health and Labour Sciences Research Grants on Ataxic Diseases (HM) of the Japanese Ministry of Health, Labour and Welfare, Japan, and by a Grant-in-Aid for Scientific Research on Innovative Areas (Comprehensive Brain Science Network) from the Ministry of Education, Science, Sports and Culture of Japan (SM).

The authors thank Mr. Noboru Ando and Mrs. Hitomi Matsuo (Tokyo Medical and Dental University) for their excellent technical assistance.

AUTHOR CONTRIBUTIONS

M. Takahashi, the first author, performed research, analyzed data and wrote the manuscript, while four others (NS, MO, YN and TI) partly performed research, and seven others (MY, HT, TK, OM, M. Takao, SM and YE) performed neuropathological examinations and assisted pathological analysis of this study, HM organized and arranged the whole project and KI designed, directed and wrote this work.

REFERENCES

1. Ishikawa K, Tanaka H, Saito M *et al.* Japanese families with autosomal dominant pure cerebellar ataxia map to chromosome 19p13.1-p13.2 and are strongly associated with mild CAG expansions in the spinocerebellar ataxia type 6 gene in chromosome 19p13.1. *Am J Hum Genet* 1997; **61**: 336–346.
2. Gomez CM, Thompson RM, Gammack JT *et al.* Spinocerebellar ataxia type 6: gaze-evoked and vertical nystagmus, Purkinje cell degeneration, and variable age of onset. *Ann Neurol* 1997; **42**: 933–950.
3. Zhuchenko O, Bailey J, Bonnen P *et al.* Autosomal dominant cerebellar ataxia (SCA6) associated with small polyglutamine expansions in the alpha 1A-voltage-dependent calcium channel. *Nat Genet* 1997; **15**: 62–69.
4. Ishikawa K, Fujigasaki H, Saegusa H *et al.* Abundant expression and cytoplasmic aggregations of [alpha]1A voltage-dependent calcium channel protein associated with neurodegeneration in spinocerebellar ataxia type 6. *Hum Mol Genet* 1999; **8**: 1185–1193.
5. Ishikawa K, Owada K, Ishida K *et al.* Cytoplasmic and nuclear polyglutamine aggregates in SCA6 Purkinje cells. *Neurology* 2001; **56**: 1753–1756.
6. Yabe I, Sasaki H, Matsuura T *et al.* SCA6 mutation analysis in a large cohort of the Japanese patients with late-onset pure cerebellar ataxia. *J Neurol Sci* 1998; **156**: 89–95.
7. Takahashi H, Ishikawa K, Tsutsumi T *et al.* A clinical and genetic study in a large cohort of patients with spinocerebellar ataxia type 6. *J Hum Genet* 2004; **49**: 256–264.
8. Orr HT, Zoghbi HY. Trinucleotide repeat disorders. *Annu Rev Neurosci* 2007; **30**: 575–621.
9. DiFiglia M, Sapp E, Chase KO *et al.* Aggregation of huntingtin in neuronal intranuclear inclusions and dystrophic neurites in brain. *Science* 1997; **277**: 1990–1993.
10. Paulson HL, Perez MK, Trottier Y *et al.* Intranuclear inclusions of expanded polyglutamine protein in spinocerebellar ataxia type 3. *Neuron* 1997; **19**: 333–344.
11. Binder DK, Scharfman HE. Brain-derived neurotrophic factor. *Growth Factors* 2004; **22**: 123–131.
12. Ferrer I, Goutan E, Marin C, Rey MJ, Ribalta T. Brain-derived neurotrophic factor in Huntington disease. *Brain Res* 2000; **866**: 257–261.
13. Zuccato C, Cattaneo E. Role of brain-derived neurotrophic factor in Huntington's disease. *Prog Neurobiol* 2007; **81**: 294–330.
14. Zuccato C, Ciammola A, Rigamonti D *et al.* Loss of huntingtin-mediated BDNF gene transcription in Huntington's disease. *Science* 2001; **293**: 493–498.
15. Gharami K, Xie Y, An JJ, Tonegawa S, Xu B. Brain-derived neurotrophic factor over-expression in the forebrain ameliorates Huntington's disease phenotypes in mice. *J Neurochem* 2008; **105**: 369–379.
16. Steffan JS, Kazantsev A, Spasic-Boskovic O *et al.* The Huntington's disease protein interacts with p53 and CREB-binding protein and represses transcription. *Proc Natl Acad Sci USA* 2000; **97**: 6763–6768.
17. Nucifora FC, Jr, Sasaki M, Peters MF *et al.* Interference by huntingtin and atrophin-1 with cbp-mediated transcription leading to cellular toxicity. *Science* 2001; **291**: 2423–2428.
18. McCampbell A, Taylor JP, Taye AA *et al.* CREB-binding protein sequestration by expanded polyglutamine. *Hum Mol Genet* 2000; **9**: 2197–2202.
19. Ishiguro T, Ishikawa K, Takahashi M *et al.* The carboxy-terminal fragment of alpha(1A) calcium channel preferentially aggregates in the cytoplasm of human spinocerebellar ataxia type 6 Purkinje cells. *Acta Neuropathol* 2010; **119**: 447–464.
20. Dieni S, Rees S. Distribution of brain-derived neurotrophic factor and TrkB receptor proteins in the fetal and postnatal hippocampus and cerebellum of the guinea pig. *J Comp Neurol* 2002; **454**: 229–240.
21. Gauthier LR, Charrin BC, Borrell-Pages M *et al.* Huntingtin controls neurotrophic support and survival of neurons by enhancing BDNF vesicular transport along microtubules. *Cell* 2004; **118**: 127–138.
22. Miyashita T, Tabuchi A, Fukuchi M *et al.* Interference with activity-dependent transcriptional activation of BDNF gene depending upon the expanded polyglutamines in neurons. *Biochem Biophys Res Commun* 2005; **333**: 1241–1248.
23. Hourez R, Servais L, Orduz D *et al.* Aminopyridines correct early dysfunction and delay neurodegeneration in a mouse model of spinocerebellar ataxia type 1. *J Neurosci* 2011; **31**: 11795–11807.

24. Schindowski K, Belarbi K, Buee L. Neurotrophic factors in Alzheimer's disease: role of axonal transport. *Genes Brain Behav* 2008; **7** (Suppl 1): 43–56.
25. Howells DW, Porritt MJ, Wong JY *et al.* Reduced BDNF mRNA expression in the Parkinson's disease substantia nigra. *Exp Neurol* 2000; **166**: 127–135.
26. Ishikawa K, Watanabe M, Yoshizawa K *et al.* Clinical, neuropathological, and molecular study in two families with spinocerebellar ataxia type 6 (SCA6). *J Neurol Neurosurg Psychiatry* 1999; **67**: 86–89.
27. Matsuda N, Lu H, Fukata Y *et al.* Differential activity-dependent secretion of brain-derived neurotrophic factor from axon and dendrite. *J Neurosci* 2009; **29**: 14185–14198.
28. Kawamoto Y, Nakamura S, Nakano S, Oka N, Akiguchi I, Kimura J. Immunohistochemical localization of brain-derived neurotrophic factor in adult rat brain. *Neuroscience* 1996; **74**: 1209–1226.
29. Kawamoto Y, Nakamura S, Kawamata T, Akiguchi I, Kimura J. Cellular localization of brain-derived neurotrophic factor-like immunoreactivity in adult monkey brain. *Brain Res* 1999; **821**: 341–349.
30. Murer MG, Boissiere F, Yan Q *et al.* An immunohistochemical study of the distribution of brain-derived neurotrophic factor in the adult human brain, with particular reference to Alzheimer's disease. *Neuroscience* 1999; **88**: 1015–1032.
31. Adachi N, Kohara K, Tsumoto T. Difference in trafficking of brain-derived neurotrophic factor between axons and dendrites of cortical neurons, revealed by live-cell imaging. *BMC Neurosci* 2005; **6**: 42.
32. Kuczewski N, Porcher C, Lessmann V, Medina I, Gaiarsa JL. Activity-dependent dendritic release of BDNF and biological consequences. *Mol Neurobiol* 2009; **39**: 37–49.

Neurobiology of Aging 34 (2013) 1101–1104

Contents lists available at SciVerse ScienceDirect

Neurobiology of Aging

journal homepage: www.elsevier.com/locate/neuaging

Brief communication

Suspected limited efficacy of γ-secretase modulators

Nobuto Kakuda [a,b], Kohei Akazawa [c], Hiroyuki Hatsuta [d], Shigeo Murayama [d], Yasuo Ihara [a,b,e,f,*], The Japanese Alzheimer's Disease Neuroimaging Initiative

[a] Department of Neuropathology, Faculty of Life and Medical Sciences, Doshisha University, Kyoto, Japan
[b] Core Research for Evolutional Science and Technology (CREST), Japan Science and Technology Agency, Saitama, Japan
[c] Department of Medical Informatics, Niigata University Medical and Dental Hospital, Niigata University, Niigata, Japan
[d] Department of Neuropathology, Tokyo Metropolitan Institute of Gerontology, Tokyo, Japan
[e] Center for Neurologic Diseases, Doshisha University, Kyoto, Japan
[f] New Energy and Industrial Technology Development Organization (NEDO), Kanagawa, Japan

ARTICLE INFO

Article history:
Received 16 June 2012
Accepted 25 August 2012
Available online 9 October 2012

Keywords:
γ-Secretase
γ-Modulator
Alzheimer's disease

ABSTRACT

Mild cognitive impairment and Alzheimer's disease (AD) are associated with changes in γ-secretase activity in the brain, producing an amyloid β-protein-42-lowering γ-modulator-like effect. We show here that this modulation occurs at the stage of amyloid deposition, presumably decades earlier than the onset of AD. In addition, γ-secretase modulator-1, a γ-modulator, altered γ-secretase activity in the AD brain but to a lesser extent than in the normal brain. These findings suggest that γ-modulators have limited efficacy against amyloid deposition and AD.

1. Introduction

Amyloid β-protein (Aβ) is cleaved sequentially from amyloid precursor protein by β- and γ-secretases (for a review see Selkoe, 2001). The longer but minor species, Aβ42, predominates in senile plaques (Iwatsubo et al., 1994). γ-Secretase, a heterogeneous complex (Takasugi et al., 2003; Serneels et al., 2009), governs the intramembrane proteolysis of type I membrane proteins including amyloid precursor protein (Sisodia and St George-Hyslop, 2002; Wakabayashi and De Strooper, 2008). We found recently that γ-secretase activity is altered in brains affected by mild cognitive impairment (MCI) or Alzheimer's disease (AD). The change decreases the concentrations of both Aβ42 and Aβ43 in cerebrospinal fluid (CSF) in patients affected with MCI or AD. To compensate for these decreases, the levels of Aβ38 and Aβ40 are increased (Kakuda et al., 2012). We assume that Aβ42 and Aβ43 are enhanced to be converted by stepwise processing to Aβ38 and Aβ40, respectively, by altered γ-secretase in the brain affected by MCI or AD (Kakuda et al., 2012; Takami et al., 2009). Reciprocal changes in the levels of Aβ42 and Aβ38 without a change in the total Aβ level are an essential characteristic of γ-secretase modulators, drugs whose development receives intense attention.

2. Materials and methods

2.1. Subjects

Human cortical specimens for quantification of raft-associated γ-secretase activity were obtained from brains that had been removed, processed, and stored at −80 °C within 12 hours postmortem; the bodies had been placed in a cold (4 °C) room within 2 hours after death. The specimens were kept at the Brain Bank at Tokyo Metropolitan Institute of Gerontology. For all the brains registered at the bank we obtained written informed consent for their use for medical research from the patient or the patient's family. Each brain specimen (approximately 0.5 g) was taken from Brodmann areas 9–11 of 13 AD patients (80 ± 5.0 years of age; Braak neurofibrillary tangle [NFT] stage >IV; senile plaque [SP] stage = C; retrospective clinical dementia rating [CDR] >1), 10 SP stage B patients (76 ± 4.0 years of age; Braak NFT stage >I; retrospective CDR = 0), 10 SP stage A patients (76 ± 4.7 years of age; Braak NFT stage >0; retrospective CDR = 0), and 16 controls in SP stage 0 (77 ± 6.5 years of age; Braak NFT stage <I; retrospective CDR = 0). SP stages were determined by modified methenamine silver stain: stage A: Aβ deposits in the basal portions of the isocortex; stage B: Aβ deposits in virtually all isocortical association

* Corresponding author at: Department of Neuropathology, Faculty of Life and Medical Sciences, Doshisha University, 4-1-1, Kizugawadai, Kizugawa, Kyoto 619-0225, Japan. Tel.: +81 774 65 6058; fax: +81 3 5800 6852.
E-mail address: yihara@mail.doshisha.ac.jp (Y. Ihara).

0197-4580/$ – see front matter © 2013 Elsevier Inc. All rights reserved.
http://dx.doi.org/10.1016/j.neurobiolaging.2012.08.017

areas except primary centers; stage C (AD): Aβ deposits in all areas of the isocortex including primary motor and sensory centers (Braak and Braak, 1991).

2.2. Quantification of brain raft-associated γ-secretase activity

A previously reported assay method was employed with some modifications (Kakuda et al., 2012). Briefly, each raft fraction, adjusted to 100 μg/mL in protein concentration, was incubated with 200 nM of βCTF-FLAG for 1 hour at 37 °C in the presence of 0, or 0.1–0.5 μM γ-secretase modulator (GSM)-1 (kindly provided by Dr M. Okochi, Osaka University). After incubation, all samples were centrifuged at 265,000*g* on a TLA110 rotor (Beckman, Palo Alto, CA, USA) for 20 minutes at 4 °C. The supernatants were separated on sodium dodecyl sulfate polyacylamide gel electrophoresis (SDS-PAGE), and subjected to quantitative Western blot analysis, using specific antibodies, 3B1 for Aβ38, BA27 for Aβ40, 44A3 for Aβ42, and anti-Aβ43 polyclonal for Aβ43.

2.3. GSM-1-induced shift of ln(Aβ38/42)

Shifts of ln(Aβ38/42) with GSM-1 were calculated as GSM-1-induced ln(Aβ38/42) minus the ratio measured in its absence.

2.4. Statistical analysis

All statistical analyses were performed using SPSS version 14.0. Data transformation was required to achieve normal distributions; all analyses were performed after logarithmic transformation of the data for Aβ38, Aβ40, Aβ42, and Aβ43. Analysis of variance was used to test the equality of mean values for continuous variables between the 4 groups: control, SP stage A, SP stage B, and AD. Multiple comparisons were made using Bonferroni *t* test to test the differences between controls, SP stage A, SP stage B, and AD. The paired *t* test was used to examine the effect of GSM-1 treatment. *p* values <0.05 were considered significant.

3. Results

We speculated that this modulation in the γ-secretase activity occurs much earlier than the onset of AD because lower Aβ42 concentrations in CSF appear to be associated with amyloid deposition itself (Fagan et al., 2006). To confirm this, we measured the activities of raft-associated γ-secretase prepared from autopsied brains using a previously established method (Kakuda et al., 2012). Raft fractions were prepared from control and AD brains (Brodmann areas 9–11), which were judged histochemically to be in the Braak SP stage 0, stage A, stage B, or stage C (AD) (Braak and Braak, 1991). Aβs produced by γ-secretase from each brain specimen were analyzed by quantitative Western blot, and the ln(Aβ40/43) and ln(Aβ38/42) ratios were obtained. Stage A plots nearly superimposed with control plots (Fig. 1; 0 vs. A: $p = 1.000$ for ln(Aβ40/43), $p = 1.000$ for ln(Aβ38/42)). However, the γ-secretase activities differed between stage B specimens and 0/A specimens (0 vs. B: $p = 0.005$ for ln(Aβ40/43) and $p < 0.001$ for ln(Aβ38/42); A vs. B: $p = 0.002$ for ln(Aβ40/43) and $p = 0.001$ for ln(Aβ38/42); Fig. 1). AD (stage C) plots were shifted the most (0 vs. C: $p < 0.001$ for ln(Aβ40/43) and $p = 0.003$ for ln(Aβ38/42); A vs. C: $p < 0.001$ for ln(Aβ40/43) and $p = 0.007$ for ln(Aβ38/42)). Most interestingly, although AD plots were shifted to the same extent as stage B plots for Aβ38/42 (B vs. C: $p = 1.000$ for ln(Aβ38/42)), stage B and AD plots differ for Aβ40/43 (B vs. C: $p < 0.001$ for ln(Aβ40/43); Fig. 1).

Although these data were obtained from a cross-sectional study, one might assume that stage A develops through to stage B and eventually to stage C over decades (Duyckaerts and Hauw, 1997).

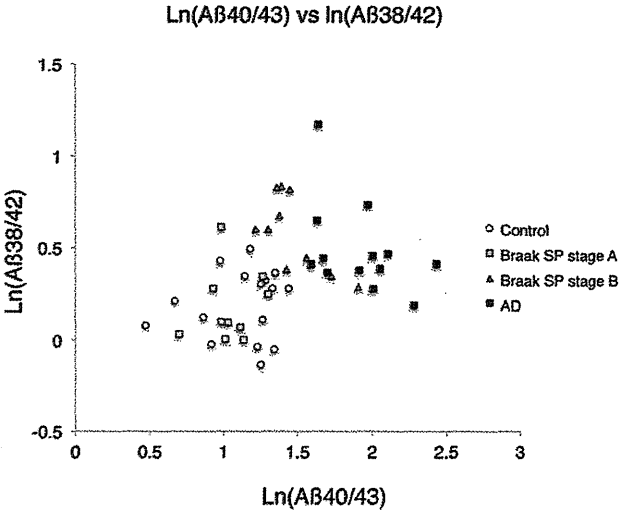

Fig. 1. Ln(amyloid-β protein [Aβ]40/43) versus ln(Aβ38/42) plot of raft-associated γ-secretase prepared from the brains in various (Braak) senile plaque (SP) stages. The raft-associated γ-secretase prepared from Braak SP stages 0, A, B, and C (AD) brain specimens were incubated with 200 nM of βCTF for 1 hour at 37 °C. After centrifugation of the reaction mixtures, the supernatants were saved for quantitative Western blot analysis of Aβs using specific antibodies.

Thus, the Aβ42 product line of γ-secretase appears to undergo changes early and the Aβ42-lowering activity remains constant through to development of AD. By contrast, the Aβ40 product line gradually changes with increasing Aβ40/43 ratio, as stage 0/A develops to stage B and finally to AD. Our previous observations showed that Aβ42 levels in CSF parallel the Aβ38/42 ratio, and Aβ43 levels parallel the Aβ40/43 ratio (Kakuda et al., 2012). These findings suggest that a decrease in the Aβ42 level would be the first alteration observable in CSF and that the level does not change throughout the disease course, whereas the Aβ43 level in CSF would decrease progressively up to AD.

We noted previously that the effects of Aβ42-lowering γ-modulators could be minimal in sporadic MCI/AD patients because modulation of γ-secretase has already begun in their brains. As mentioned above, the modulation of γ-secretase is evident in stage B. Accordingly, we investigated the response of γ-secretase to GSM-1, an Aβ42-lowering modulator, in control and AD brains. We reasoned that a strong response of the altered γ-secretase to GSM-1 would indicate that the drug might still be effective.

We quantified γ-secretase activities in the absence or presence of GSM-1 in control and AD specimens. This agent is known to aggressively modulate only conversion from Aβ42 to Aβ38, but not that from Aβ43 to Aβ40 (Crump et al., 2011; Ebke et al., 2011; Ohki et al., 2011). As expected, GSM-1 treatment significantly lowered Aβ42 and increased Aβ38 in control (see Supplementary Fig. 1). By contrast, in AD specimens, GSM-1 lowered Aβ42 and increased Aβ38 but to a lesser extent (Supplementary Fig. 1). The generation of Aβ40 and Aβ43, and the total production of Aβ were unchanged by the treatment of GSM-1 in all specimens (Supplementary Fig. 1).

In AD specimens, conversion of Aβ43 to Aβ40 seems to be altered compared with control (Kakuda et al., 2012), but this might be due to high concentrations of GSM-1 (>0.5 μM), which suppressed Aβ40 (and Aβ43) product line and total Aβ production in both control and AD specimens (data not shown). GSM-1 treatment significantly elevated the ratio of Aβ38/42 in control (Aβ38/42 with dimethyl sulfoxide vs. Aβ38/42 with GSM-1; $p < 0.000$, paired *t* test; Fig. 2A). By contrast, the same treatment of AD specimens

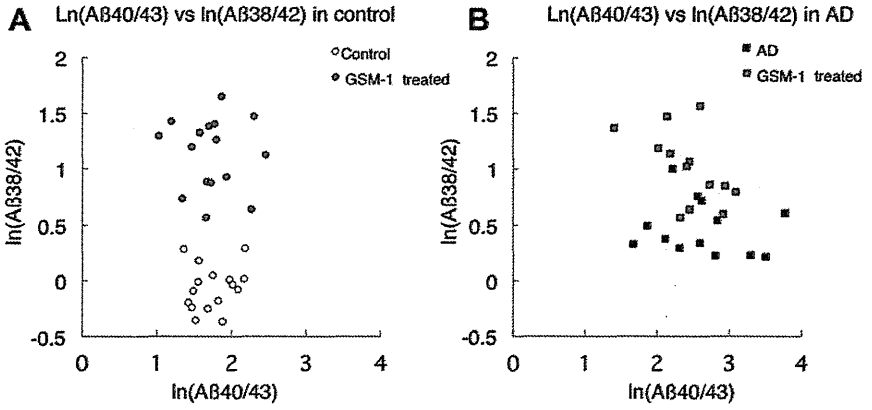

Fig. 2. Ln(amyloid-β protein [Aβ]40/43) versus ln(Aβ38/42) plot of γ-secretase modulator (GSM)-1-treated raft-associated γ-secretase activity. The raft-associated γ-secretases prepared from control (A) and AD (B) brains were incubated with 200 nM of βCTF for 1 hour at 37 °C in the presence of dimethyl sulfoxide or 0.3 μM GSM-1. Aβs produced were quantified by quantitative Western blot analysis using specific antibodies.

caused a much smaller increase in the Aβ38/42 ratio ($p < 0.001$ for AD paired t test; Fig. 2B). There was no significant difference in the Aβ40/43 ratio between control and AD specimens (Aβ40/43 with dimethyl sulfoxide vs. Aβ40/43 with GSM-1; $p = 0.814$ for control; $p = 0.223$ for AD, respectively; paired t test; Fig. 2A and B). The modulating effect on the Aβ38/42 ratio can be interpreted as indicating the extent of GSM-1-induced shift in the Aβ38/42 ratio (Supplementary Table 1). γ-Secretase was associated with significantly lower ratios in AD specimens than in control specimens (control vs. AD: $p < 0.001$), indicating a poor response to GSM-1 in AD specimens.

4. Discussion

Modulation of γ-secretase occurs in AD brains (Kakuda et al., 2012), and to a significant extent already at the stage of amyloid deposition, a decade or even decades before the onset of AD (Duyckaerts and Hauw, 1997). Although γ-secretase self-modulates and produces less Aβ42, it is likely that β-amyloid accumulation slowly progresses and ultimately extends throughout the brain, finally involving primary cortical centers (Duyckaerts and Hauw, 1997). A gradual decline in the rate of Aβ accumulation curve (Kawarabayashi et al., 2001) might be caused by self-modulation of γ-secretase. Currently, we do not know which comes first, Aβ deposition or γ-self-modulation. However, the efficacy of GSM-1 and γ-modulators in general would be limited when Aβ42 deposition and self-modulation of γ-secretase begins in the brain. To date, the efficacy of γ-modulators has been confirmed most often using younger Tg2576 mice, which do not yet accumulate Aβ (Borgegard et al., 2012; Kounnas et al., 2010). In Tg2576 mice, Aβ deposition starts at 9–12 months, and γ-secretase activity changes together with increasing Aβ deposition in the brain starting at 15–16 months of age (Kawarabayashi et al., 2001; data not shown). Thus, the true effectiveness of γ-modulators in Tg2576 mice should be assessed after 15–16 months of age. It is unclear whether γ-modulators are effective in such amyloid-bearing aged mice.

Disclosure statement

The authors have no conflict of interest.

Ethic permission was approved by Faculty of Life and Medical Sciences, Doshisha University, and we obtained written informed consent for their use for medical research from the patient or the patient's family.

Acknowledgements

The authors thank Dr Masayasu Okochi, Neuropsychiatry and Neurochemistry, Department of Integrated Medicine, Osaka University Graduate School of Medicine, for kindly providing GSM-1, and Dr Satoru Funamoto, Department of Neuropathology, Faculty of Life and Medical Sciences, Doshisha University, for providing βCTF. This project was supported in part by the New Energy and Industrial Technology Development Organization, Japan (J-ADNI) and by the MEXT-Supported Program for the Strategic Research Foundation at Private Universities, 2012–2017.

Appendix A. Supplementary data

Supplementary data associated with this article can be found, in the online version, at http://dx.doi.org/10.1016/j.neurobiolaging.2012.08.017.

References

Borgegard, T., Juréus, A., Olsson, F., Rosqvist, S., Sabirsh, A., Rotticci, D., Paulsen, K., Klintenberg, R., Yan, H., Waldman, M., Stromberg, K., Nord, J., Johansson, J., Regner, A., Parpal, S., Malinowsky, D., Radesater, A.C., Li, T., Singh, R., Eriksson, H., Lundkvist, J., 2012. First and second generation γ-secretase modulators (GSMs) modulate amyloid-β (Aβ) peptide production through different mechanisms. J. Biol. Chem. 287, 11810–11819.

Braak, H., Braak, E., 1991. Neuropathological stageing of Alzheimer-related changes. Acta Neuropathol. 82, 239–259.

Crump, C.J., Fish, B.A., Castro, S.V., Chau, D.M., Gertsik, N., Ahn, K., Stiff, C., Pozdnyakov, N., Bales, K.R., Johnson, D.S., Li, Y.M., 2011. Piperidine acetic acid based γ-secretase modulators directly bind to Presenilin-1. ACS Chem. Neurosci. 2, 705–710.

Duyckaerts, C., Hauw, J.J., 1997. Prevalence, incidence and duration of Braak's stages in the general population: can we know? Neurobiol. Aging 18, 362–369.

Ebke, A., Luebbers, T., Fukumori, A., Shirotani, K., Haass, C., Baumann, K., Steiner, H., 2011. Novel γ-secretase enzyme modulators directly target presenilin protein. J. Biol. Chem. 286, 37181–37186.

Fagan, A.M., Mintun, M.A., Mach, R.H., Lee, S.Y., Dence, C.S., Shah, A.R., LaRossa, G.N., Spinner, M.L., Klunk, W.E., Mathis, C.A., DeKosky, S.T., Morris, J.C., Holtzman, D.M., 2006. Inverse relation between in vivo amyloid imaging load and cerebrospinal fluid Abeta42 in humans. Ann. Neurol. 59, 512–519.

Iwatsubo, T., Odaka, A., Suzuki, N., Mizusawa, H., Nukina, N., Ihara, Y., 1994. Visualization of Aβ42(43) and Aβ40 in senile plaque with end-specific Aβ monoclonals: evidence that an initially deposited forms is Aβ42(43). Neuron 13, 45–53.

Kakuda, N., Shoji, M., Arai, H., Furukawa, K., Ikeuchi, T., Akazawa, K., Takami, M., Hatsuta, H., Murayama, S., Hashimoto, Y., Miyajima, M., Arai, H., Nagashima, Y., Yamaguchi, H., Kuwano, R., Nagaike, K., Ihara, Y., Japanese Alzheimer's Disease Neuroimaging Initiative, 2012. Altered γ-secretase activity in mild cognitive impairment and Alzheimer's disease. EMBO Mol. Med. 4, 344–352.

Kawarabayashi, T., Younkin, L.H., Saido, T.C., Shoji, M., Ashe, K.H., Younkin, S.G., 2001. Age-dependent changes in brain, CSF, and plasma amyloid (β) protein in the Tg2576 transgenic mouse model of Alzheimer's disease. J. Neurosci. 21, 372–381.

Kounnas, M.Z., Danks, A.M., Cheng, S., Tyree, C., Ackerman, E., Zhang, X., Ahn, K., Nguyen, P., Comer, D., Mao, L., Yu, C., Pleynet, D., Digregorio, P.J., Velicelebi, G., Stauderman, K.A., Comer, W.T., Mobley, W.C., Li, Y.M., Sisodia, S.S., Tanzi, R.E., Wagner, S.L., 2010. Modulation of gamma-secretase reduces beta-amyloid deposition in a transgenic mouse model of Alzheimer's disease. Neuron 67, 769–780.

Ohki, Y., Higo, T., Uemura, K., Shimada, N., Osawa, S., Berezovska, O., Yokoshima, S., Fukuyama, T., Tomita, T., Iwatsubo, T., 2011. Phenylpiperidine-type γ-secretase modulators target the transmembrane domain 1 of presenilin 1. EMBO J. 30, 4815–4824.

Selkoe, D.J., 2001. Alzheimer's disease: genes, proteins, and therapy. Physiol. Rev. 81, 741–766.

Serneels, L., Van Biervliet, J., Craessaerts, K., Dejaegere, T., Horré, K., Van Houtvin, T., Esselmann, H., Paul, S., Schäfer, M.K., Berezovska, O., Hyman, B.T., Sprangers, B., Sciot, R., Moons, L., Jucker, M., Yang, Z., May, P.C., Karran, E., Wiltfang, J., D'Hooge, R., De Strooper, B., 2009. γ-Secretase heterogeneity in the Aph1 subunit: relevance for Alzheimer's disease. Science 324, 639–642.

Sisodia, S.S., St George-Hyslop, P.H., 2002. gamma-Secretase, Notch, Abeta and Alzheimer's disease: where do the presenilins fit in? Nat. Rev. Neurosci. 3, 281–290.

Takami, M., Nagashima, Y., Sano, Y., Ishihara, S., Morishima-Kawashima, M., Funamoto, S., Ihara, Y., 2009. γ-Secretase: successive tripeptide and tetrapeptide release from the transmembrane domain of β-carboxyl terminal fragment. J. Neurosci. 29, 13042–13052.

Takasugi, N., Tomita, T., Hayashi, I., Tsuruoka, M., Niimura, M., Takahashi, Y., Thinakaran, G., Iwatsubo, T., 2003. The role of presenilin cofactors in the γ-secretase complex. Nature 422, 438–441.

Wakabayashi, T., De Strooper, B., 2008. Presenilins: members of the gamma-secretase quartets, but part-time soloists too. J. Physiol. 23, 194–204.

BMJ open accessible medical research

Multicentre multiobserver study of diffusion-weighted and fluid-attenuated inversion recovery MRI for the diagnosis of sporadic Creutzfeldt–Jakob disease: a reliability and agreement study

Koji Fujita,[1] Masafumi Harada,[2] Makoto Sasaki,[3] Tatsuhiko Yuasa,[4] Kenji Sakai,[5] Tsuyoshi Hamaguchi,[5] Nobuo Sanjo,[6] Yusei Shiga,[7] Katsuya Satoh,[8] Ryuichiro Atarashi,[8] Susumu Shirabe,[9] Ken Nagata,[10] Tetsuya Maeda,[10] Shigeo Murayama,[11] Yuishin Izumi,[1] Ryuji Kaji,[1] Masahito Yamada,[5] Hidehiro Mizusawa[6]

To cite: Fujita K, Harada M, Sasaki M, *et al*. Multicentre, multiobserver study of diffusion-weighted and fluid-attenuated inversion recovery MRI for the diagnosis of sporadic Creutzfeldt–Jakob disease: a reliability and agreement study. *BMJ Open* 2012;**2**: e000649. doi:10.1136/bmjopen-2011-000649

► Prepublication history for this paper is available online. To view this file please visit the journal online (http://bmjopen.bmj.com).

Received 21 November 2011
Accepted 20 December 2011

For numbered affiliations see end of article.

Correspondence to
Dr Masafumi Harada;
masafumi@clin.med.tokushima-u.ac.jp

ABSTRACT

Objectives: To assess the utility of the display standardisation of diffusion-weighted MRI (DWI) and to compare the effectiveness of DWI and fluid-attenuated inversion recovery (FLAIR) MRI for the diagnosis of sporadic Creutzfeldt–Jakob disease (sCJD).

Design: A reliability and agreement study.

Setting: Thirteen MRI observers comprising eight neurologists and five radiologists at two universities in Japan.

Participants: Data of 1.5-Tesla DWI and FLAIR were obtained from 29 patients with sCJD and 13 controls.

Outcome measures: Standardisation of DWI display was performed utilising b0 imaging. The observers participated in standardised DWI, variable DWI (the display adjustment was observer dependent) and FLAIR sessions. The observers independently assessed each MRI for CJD-related lesions, that is, hyperintensity in the cerebral cortex or striatum, using a continuous rating scale. Performance was evaluated by the area under the receiver operating characteristics curve (AUC).

Results: The mean AUC values were 0.84 (95% CI 0.81 to 0.87) for standardised DWI, 0.85 (95% CI 0.82 to 0.88) for variable DWI and 0.68 (95% CI 0.63 to 0.72) for FLAIR, demonstrating the superiority of DWI ($p<0.05$). There was a trend for higher intraclass correlations of standardised DWI (0.74, 95% CI 0.66 to 0.83) and variable DWI (0.72, 95% CI 0.62 to 0.81) than that of FLAIR (0.63, 95% CI 0.53 to 0.74), although the differences were not statistically significant.

Conclusions: Standardised DWI is as reliable as variable DWI, and the two DWI displays are superior to FLAIR for the diagnosis of sCJD. The authors propose that hyperintensity in the cerebral cortex or striatum on 1.5-Tesla DWI but not FLAIR can be a reliable diagnostic marker for sCJD.

ARTICLE SUMMARY

Article focus

- Evaluation of the reliability of diffusion-weighted imaging (DWI) display standardisation for the diagnosis of sporadic Creutzfeldt–Jakob disease (sCJD).
- Comparison between DWI and fluid-attenuated inversion recovery (FLAIR) for the diagnosis of sCJD.

Key messages

- Standardised DWI display is as reliable as observer-dependent DWI display.
- DWI is superior to FLAIR for the diagnosis of sCJD.
- Hyperintensity in the cerebral cortex or striatum on 1.5-Tesla DWI but not FLAIR can be a reliable diagnostic marker for sCJD.

Strengths and limitations of this study

- Strength of this study is the large number of physicians who participated in the observer performance study.
- This study was limited by the retrospective nature that may lead to a selection bias.

INTRODUCTION

Reliable detection of Creutzfeldt–Jakob disease (CJD) is imperative for infection control and treatment. MRI is useful for the early diagnosis of CJD,[1 2] whereas the utility of EEG and conventional cerebrospinal fluid (CSF) tests have been limited.[3] Diffusion-weighted imaging (DWI) and fluid-attenuated inversion recovery (FLAIR) are key techniques for the diagnosis of sporadic CJD (sCJD) with high sensitivity and specificity when assessed by expert neurologists or

neuroradiologists.[1 4 5] However, the utility of MRI for general neurologists or radiologists who are not familiar with diagnosing CJD remains elusive. Moreover, standardisation of MRI methodologies, which would be essential for the reproducible assessment of MRI findings of CJD cases, has not been achieved in previous studies.[1 4 5] DWI display conditions may particularly vary among institutions or operators,[6] which can give rise to inaccurate assessment of CJD-related lesions, specifically subtle abnormalities in the cerebral cortex. Meanwhile, although DWI seems superior to FLAIR for the detection of CJD lesions,[5] direct comparison of the two sequences is yet to be performed.

To address these issues, we investigated the utility of a newly proposed standardisation method of DWI display[6 7] and compared the effectiveness of DWI and FLAIR for the diagnosis of sCJD, particularly for differentiating between abnormal and normal signals by neurologists and radiologists who are not necessarily CJD experts. We conducted a multicentre, multiobserver case–control study and evaluated observer performance with receiver operating characteristics (ROC) analysis.

METHODS

Subjects

Patients diagnosed as having sCJD by the CJD Surveillance Committee of Japan[8] from October 2005 to September 2010 were eligible to participate in this study. The accuracy of the diagnosis was defined as follows: definite, that is, pathologically verified cases; probable, that is, cases with neuropsychiatric manifestations compatible with sCJD and periodic sharp wave complexes on EEG without pathological examinations and possible, that is, cases with the same findings as probable sCJD but no periodic sharp wave complexes on EEG.[8 9] WHO criteria[10] were not applied because the assay of CSF 14-3-3 protein, which is required by WHO criteria, was standardised only since April 2009 in Japan.[11] The prion protein gene (*PRNP*) was analysed in the open reading frame after extracting DNA from patients' blood.[12 13] For neuropathological examinations, brain sections were stained with routine techniques, and immunohistochemistry was performed using the mouse monoclonal antibody 3F4 (Senetek, MD Heights, Missouri, USA).[12] For PrP^{Sc} typing, frozen brain tissues were homogenised and analysed by western blot for proteinase K-resistant PrP using the 3F4 antibody.[14] Assays for CSF γ-isoform of 14-3-3 protein,[11] total τ protein (cut-off value, 1300 pg/ml)[15] and real-time quaking-induced conversion (RT-QUIC)[16] were performed in patients whose CSF samples were available. The following patients were eligible as disease controls: patients who were suspected to have prion disease by primary physicians but were denied to have prion disease by the Committee or those who were diagnosed as having other neurological disorders at Tokushima University Hospital and whose brain MRI showed no abnormal intensity in the cerebral cortex or striatum. We requested physicians who had referred patients to the Committee to provide initial MRI data of eligible patients.

This study was approved by the Medical Ethics Committee of Kanazawa University and the Ethics Committees of the Tokushima University Hospital and Tokyo Medical and Dental University. Written informed consent was obtained from all patients or their families.

Magnetic resonance imaging

DWI, b0 and FLAIR images were converted to the Digital Imaging and Communication in Medicine format. When the Digital Imaging and Communication in Medicine data contained patient information, it was excluded by one of the investigators (MH) before the observer performance study. All MRI studies were performed on 1.5-Tesla scanners at each hospital. Quadrature detection head coils or multichannel head coils were used. DWI was performed using the single-shot spin-echo echo planar imaging technique with the following parameters: repetition time, 4000–8000 ms; echo time, 70–100 ms; b value, 1000 s/mm^2; slice thickness, 5 mm; matrix size, 128×80 to 128×128; field of view, 220–230 mm and 16–20 contiguous axial sections parallel to a line through the anterior and posterior commissures were obtained from each patient. The scanning parameters of FLAIR were as follows: repetition time, 8000–10 000 ms; inversion time, 2000–2500 ms; effective echo time, 105–120 ms; matrix size, 256×192 to 320×224; field of view, 210–220 mm; slice thickness, 5–6 mm with 1–1.5 mm interslice gaps and 19–20 slices per patient.

Display methods

Two display methods were used for DWI: standardised and variable. In the standardised display, the window width and level settings were constant for all evaluations and could not be changed. Details of the standardised display have been reported elsewhere.[6] In brief, the window width and level were as follows: window width = SI_{b0} and window level = $SI_{b0}/2$, where SI_{b0} represents the signal intensity in the normal-appearing subcortical region on b0 imaging.[6] One radiologist (MH) manually measured SI_{b0} within a circular region of interest. The calculated window width and level were applied to all images. In the variable display mode, regarded as the most reliable for assessment of DWI, each observer was able to change the window width and level settings on the monitor according to preference. FLAIR was assessed with the variable display method because no standardised methods are currently available for FLAIR display.

Observer performance study

Eight neurologists (6–27 years of experience; mean, 12 years; board certified, six) and five radiologists (5–25 years of experience; mean, 12.8 years; board certified, four; neuroradiologist, one) participated in the observer performance study at The University of Tokushima Graduate School (persons, six; neurologists, three) and Tokyo Medical and Dental University

(persons, seven; neurologists, five including NS and YS). Before the test, the observers were informed that the purpose of the study was to evaluate their performance in detecting MRI lesions compatible with CJD, that is, hyperintensity in the cerebral cortex or striatum, regardless of signal changes in other regions including the thalamus. Three sessions were conducted: standardised DWI, variable DWI and FLAIR. To reduce the effect of learning, the interval between reading sessions was 1 week or longer. The order of the three sessions was randomised among the observers. Using computer randomisation, images of patients with and without sCJD were intermixed. All cases were presented in the same randomised order to the observers in each session. Each observer independently viewed all slices of each MRI study on the same type of monitors (Let'snote, Panasonic, Osaka, Japan) using INTAGE Realia Professional (Cubernet, Tokyo, Japan) run on Windows XP (Microsoft). The observers were allowed to adjust the window width and level only in variable DWI and FLAIR sessions but not in the standardised DWI session. Observers were blinded to any clinical information including age, sex and diagnosis.

Each observer used a continuous rating scale of a line-marking method to rate his or her confidence level on the paper format independently. At the left end of the line, a confidence level that lesions compatible with CJD were definitely absent was indicated, whereas at the right end, a confidence level that lesions were definitely present was indicated. Intermediate levels of confidence were indicated by the different positions on the line between the two ends. The distance between the left end and the marked point was converted to a confidence level that could range from 0 to 100, as described elsewhere.[17]

Statistical analyses

Observer performance was evaluated using ROC analysis with SPSS V.19 (IBM). The ROC curves for each observer indicated the ratio of the true-positive fraction to the false-positive fraction at each confidence level. The area under the ROC curve (AUC) was used to compare observer performance for accurately detecting CJD lesions. Intraclass correlations were calculated in the neurologist group, the radiologist group and for all observers by two-way random consistency measures using the SPSS software. In all the analyses, p values of <0.05 were considered statistically significant.

RESULTS

Patients and controls

MRI data from 85 patients were provided. Of these, 42 subjects from 15 hospitals (including authors' institutions) were eligible for this study after excluding cases that were diagnosed as having non-sporadic CJD or lacked the required MRI sequences. This study cohort included 29 patients with sCJD (men, 11; mean age, 71 years; duration before MRI, 4.4±6.1 months), three patients who were suspected of CJD but eventually diagnosed as negative by the Committee and 10 patients diagnosed as having other neurological disorders. Of the 29 sCJD patients, four had definite, 24 had probable and one had possible CJD. Twenty-six cases underwent *PRNP* analysis, 24 were homozygous for methionine at codon 129 and two were heterozygous with methionine and valine at codon 129. Of the four definite cases, PrP^{Sc} was type 1 in two cases, type 1+2 in one case and type 2 in one case. Eleven of 15 CSF samples from probable sCJD cases were positive for PrP^{Sc} by RT-QUIC (table 1).

Diagnoses for three prion-denied patients were immune-mediated encephalopathy, juvenile Alzheimer's disease and frontotemporal dementia. Other neurological controls were diagnosed with Alzheimer's disease, Parkinson's disease, spinocerebellar degeneration, vascular dementia, old cerebral infarction, benign paroxysmal positional vertigo, dizziness, temporal arteritis, cervical spondylosis and diabetic neuropathy.

Diagnostic performance

We investigated the diagnostic performance of standardised DWI, variable DWI and FLAIR images assessed by eight neurologists and five radiologists using ROC analysis. Mean AUC values obtained from the three sessions were compared within the neurologist group, the radiologist group and all observers (figure 1, table 2). The AUC values for standardised and variable DWI were not different within each professional group or for the total observer group. On the other hand, AUC values for FLAIR were significantly lower than DWI displayed by either method ($p<0.05$). Representative MRI scans are shown in figure 2.

Rating agreement

To measure the extent to which the observers agreed when rating the MRI findings, intraclass correlations were calculated. The intraclass correlations of the standardised DWI (0.74, 95% CI 0.66 to 0.83) and variable DWI (0.72. 95% CI 0.62 to 0.81) tend to be higher than that of FLAIR (0.63, 95% CI 0.53 to 0.74), specifically in the neurologist group, although the differences were not significant (figure 3).

DISCUSSION

We demonstrated that standardised DWI was as useful as variable DWI and that both DWI displays are superior to FLAIR for the diagnosis of sCJD when assessed by multiobservers with various specialty backgrounds.

Our standardisation method of DWI display was originally proposed as an easy-to-use way to decide the window width and level for DWI even in emergency settings.[6] Indeed, this method was demonstrated as useful for detecting acute ischaemic lesions on DWI.[7] Results of the present study show that the standardisation method is also reliable for diagnosis of sCJD, in which DWI is one of the key sequences. We suggest some advantages of standardised DWI over variable DWI, although there was no statistical difference between the two methods. First, standardised DWI can be helpful for

Table 1 Clinical profiles of patients with sporadic Creutzfeldt–Jakob disease

No	Age/sex	Diagnosis	Codon129/PrP^{Sc}	14-3-3/total τ	RT-QUIC	Pre-MRI duration (months)
1	69/M	Definite	MM/1	+/+	+	−2*
2	77/F	Definite	MM/1	+/+	+	19
3	75/F	Definite	ND/1+2	+/+	+	3
4	65/M	Definite	MM/2	−/−	−	12
5	69/M	Probable	MM	ND	−	0.5
6	72/F	Probable	MM	ND	ND	0.5
7	77/F	Probable	MM	−/−	+	0.5
8	72/M	Probable	MM	ND	ND	1
9	63/M	Probable	MM	+/+	+	1.5
10	88/F	Probable	MM	ND	ND	1.5
11	75/M	Probable	MV	ND	ND	1.5
12	56/M	Probable	MM	+/+	+	2
13	67/M	Probable	MM	+/+	−	2
14	70/M	Probable	MM	+/+	+	2
15	70/F	Probable	MM	+/+	+	2
16	74/F	Probable	MM	+/+	−	2
17	84/F	Probable	MM	+/−	+	2
18	85/F	Probable	MM	−/+	+	2
19	49/F	Probable	ND	+/+	+	2
20	74/F	Probable	MV	+/+	+	2.5
21	54/F	Probable	ND	ND	ND	2.5
22	61/M	Probable	MM	ND	ND	3
23	72/F	Probable	MM	+/−	−	3
24	81/F	Probable	MM	−/−	+	3
25	70/M	Probable	MM	+/+	+	6
26	83/F	Probable	MM	+/+	ND	9
27	67/F	Probable	MM	+/+	−	15
28	84/F	Probable	MM	+/+	−	26
29	57/F	Possible	MM	ND	ND	4

*MRI was obtained 2 months before the symptom onset.[2]
MM, homozygous for methionine; MV, heterozygous with methionine and valine; ND, not done; RT-QUIC, real-time quaking-induced conversion.

physicians who can refer only to hardcopies but not softcopies. Second, even for doctors who can readily refer to softcopies and thus variable DWI, the standardisation method can simplify assessment procedure without any disadvantages. Third, the standardisation can facilitate direct comparison of DWI findings from different CJD patients.

DWI and FLAIR have been reported as useful markers for the diagnosis of CJD. Of these, DWI has been assumed to be the most sensitive, although without direct evidence.[1 5 18] Hyperintensity in the cerebral cortices, the striatum or both indicates the diagnosis of CJD. The striatum hyperintensity is anterior dominant at early stages of the disease.[19] MRI lesion profiles reportedly differ among molecular subtypes of sCJD,[20 21] which was not reproduced in a recent study.[5] Zerr *et al*[4] proposed that high-signal abnormalities in caudate nucleus and putamen or at least two cortical regions (temporal, parietal or occipital lobes) either in DWI or FLAIR together with typical clinical signs can be diagnostic for probable sCJD. Based partly upon their report, 'high signal in caudate/putamen on MRI brain scan' has

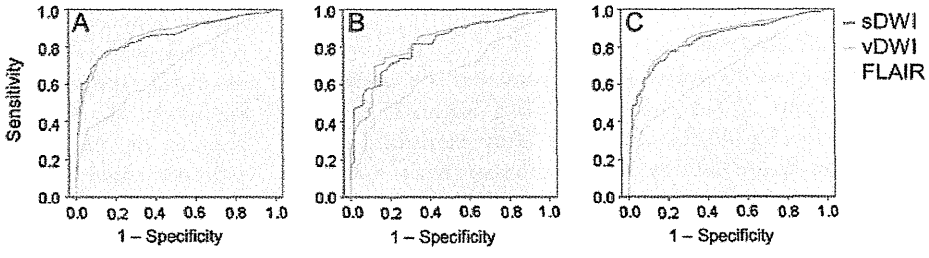

Figure 1 Receiver operating characteristic curves for each display in diagnosis of sporadic Creutzfeldt–Jakob disease. (A) Neurologists, (B) radiologists and (C) all observers. The true rate (sensitivity) is plotted as a function of the false-positive rate (1 – specificity). DWI, diffusion-weighted imaging; FLAIR, fluid-attenuated inversion recovery; sDWI, standardised DWI; vDWI, variable DWI.

Table 2 Areas under the receiver operating characteristic curves

	Neurologists	Radiologists	All observers
sDWI	0.86 (0.82 to 0.90)	0.82 (0.77 to 0.88)	0.84 (0.81 to 0.87)
vDWI	0.86 (0.82 to 0.90)	0.83 (0.77 to 0.89)	0.85 (0.82 to 0.88)
FLAIR	0.69 (0.63 to 0.75)	0.66 (0.58 to 0.73)	0.68 (0.63 to 0.72)

Means (95% CIs) are indicated.
DWI, diffusion-weighted imaging; FLAIR, fluid-attenuated inversion recovery; sDWI, standardised DWI; vDWI, variable DWI.

been used as one of the laboratory findings in the diagnostic criteria for probable sCJD in the European CJD Surveillance System (EUROCJD) since January 2010.[22] However, their criteria did not distinguish DWI and FLAIR, thereby maintaining ambiguity about the diagnostic values of MRI in situations where DWI is not available. Our data indicate that FLAIR without DWI is unreliable for the diagnosis of sCJD. On the other hand, high signals in the cerebral cortex have not been regarded as diagnostic in the EUROCJD criteria, probably because cortical abnormalities are less reliable on conventional MRI. Our results suggest that, using standardised or variable DWI but not FLAIR, cortical signals can also be used as a diagnostic marker.

Meanwhile, Young *et al*[23] reported that the sensitivity and the specificity of DWI and FLAIR for the diagnosis of CJD are 91% and 95%, respectively. More recently, Vitali *et al*[5] reported that hyperintensity greater on DWI than FLAIR is diagnostic for sCJD, whereas hyperintensity greater on FLAIR than DWI is characteristic for non-prion rapidly progressive dementia. Furthermore, reduction of apparent diffusion coefficient in subcortical (striatum) hyperintensity regions on DWI is supportive for sCJD.[5 24 25] These findings can be greatly helpful for differentiating sCJD from other rapidly progressive dementia. However, assessment of FLAIR lesions tends to vary among physicians, particularly among neurologists, as shown by the present study, and standardised methods for FLAIR or apparent diffusion coefficient map have not been established until date. Therefore, clinical criteria which require DWI but not necessarily FLAIR or apparent diffusion coefficient will be more readily applicable.

As many as 13 neurologists and radiologists from different institutions participated in the observer performance study, although the sample size of patients was relatively small. Notably, the observers had various specialty backgrounds such as stroke neurologists, neurophysiologists, experts in dementia or prion disease and general and neuroradiologists. This variety simulates practical situations in which the diagnosis of suspected CJD cases may be made by physicians who do not necessarily specialise in prion disease.

This study has some limitations. First, we did not evaluate patterns of cortical involvement suggestive of sCJD[4 5] because we had to address whether DWI or FLAIR is suitable for detecting cortical lesions in the first place. Second, we did not assess the difference among sCJD subtypes[21] because majority of our cases had a typical phenotype and were homozygous for methionine; thus, they were compatible with MM1 sCJD. Until date, MM2 thalamic-type sCJD remains a diagnostic challenge in MRI-based assessment; thalamic hypoperfusion or hypometabolism on SPECT or PET can be useful.[26] Third, majority of the control patients were not those who were suspected to have CJD. However, the

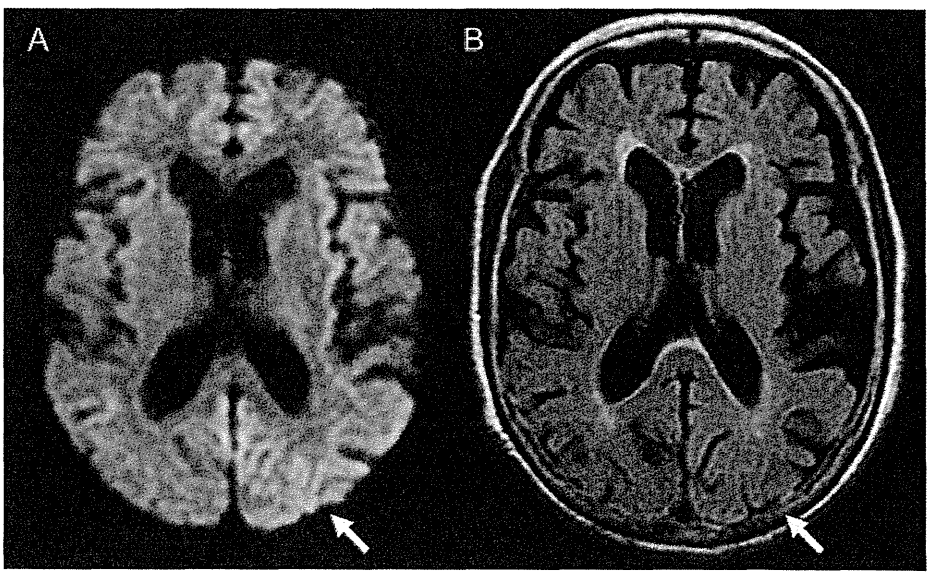

Figure 2 Representative MRI of a sporadic Creutzfeldt–Jakob disease patient (case 17). Abnormal hyperintensity in the cerebral cortex is evident on standardised diffusion-weighted imaging (A, arrow) but obscure on fluid-attenuated inversion recovery (B, arrow).

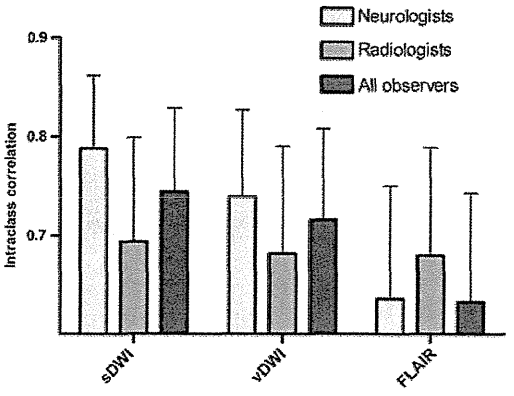

Figure 3 Intraclass correlations for each display. Error bars represent upper limits of 95% CIs. DWI, diffusion-weighted imaging; FLAIR, fluid-attenuated inversion recovery; sDWI, standardised DWI; vDWI, variable DWI.

principle aim of the present study was to establish a display method, which reliably distinguishes potentially CJD-associated signals from normal signals. Thus, our results provide a practical foundation for utilising DWI as a general diagnostic marker of sCJD when combined with previous findings.[1 4 5]

Although neuropathological confirmation of the diagnosis of sCJD was obtained in few cases, we performed RT-QUIC, a newly established CSF PrP^{Sc} amplification assay which achieved >80% sensitivity and 100% specificity for CJD.[16] Overall, 15 of 29 cases (51.7%) were pathologically proven or confirmed by RT-QUIC to have CJD. There were no significant differences in MRI findings between sCJD patients with and without positive results of CSF 14-3-3 protein, total τ protein or RT-QUIC. It will be important to further evaluate accurate diagnostic ability (sensitivity and specificity) of DWI in a prospective cohort of suspected CJD patients, that is, consecutive patients registered to the CJD surveillance who will also undergo CSF confirmation tests or neuropathological analyses.

In conclusion, we suggest that hyperintensity in the cerebral cortex or striatum assessed on the standardised or variable DWI scanned with 1.5-Tesla machines can be a reliable first-line on-site diagnostic marker for sCJD.

Author affiliations
[1]Department of Clinical Neuroscience, Institute of Health Biosciences, The University of Tokushima Graduate School, Tokushima, Japan
[2]Department of Radiology, Institute of Health Biosciences, The University of Tokushima Graduate School, Tokushima, Japan
[3]Advanced Medical Science Center, Iwate Medical University, Morioka, Japan
[4]Department of Neurology, Kamagaya-Chiba Medical Center for Intractable Neurological Disease, Kamagaya General Hospital, Kamagaya, Japan
[5]Department of Neurology and Neurobiology of Aging, Kanazawa University Graduate School of Medical Science, Kanazawa, Japan
[6]Department of Neurology and Neurological Science, Graduate School, Tokyo Medical and Dental University, Tokyo, Japan
[7]Department of Neurology, Aoba Neurosurgical Clinic, Sendai, Japan
[8]Department of Molecular Microbiology and Immunology, Nagasaki University Graduate School of Biomedical Sciences, Nagasaki, Japan
[9]Center for Health and Community Medicine, Nagasaki University, Nagasaki, Japan
[10]Department of Neurology, Research Institute for Brain and Blood Vessels, Akita, Japan
[11]Department of Neuropathology (Brain Bank for Aging Research), Tokyo Metropolitan Institute of Gerontology, Tokyo, Japan

Acknowledgements We thank Tetsuyuki Kitamoto (Tohoku University Graduate School of Medicine) for *PRNP* analysis, western blotting of PrP and neuropathological investigations; Yuka Terasawa, Yoshimitsu Shimatani, Ai Miyashiro (Department of Clinical Neuroscience, The University of Tokushima Graduate School), Hideki Otsuka, Naomi Morita, Yoichi Otomi (Department of Radiology, The University of Tokushima Graduate School), Satoru Ishibashi, Takumi Hori, Akira Machida (Department of Neurology and Neurological Science, Tokyo Medical and Dental University), Isamu Ohashi and Takashi Katayama (Department of Radiology, Tokyo Medical and Dental University) for participation in the observer performance study. We also thank Joe Senda (Nagoya University), Yuko Nemoto (Chiba Medical Center), Akio Kawakami (Kaetsu Hospital), Isao Sasaki (Mizunomiyako Memorial Hospital), Shigeyuki Kojima (Matsudo Municipal Hospital), Motohiro Yukitake (Saga University), Hiroyuki Murai (Iizuka Hospital), Hideki Mizuno (Kohnan Hospital), Akira Arai (Aomori Prefectural Central Hospital), Masamitsu Yaguchi (Shinoda General Hospital), Takanori Oikawa (South Miyagi Medical Center) and all other collaborative physicians for providing MRI data of the patients. We thank the members of the CJD Surveillance Committee of Japan for their support of this work.

Funding This study was supported by Grants-in-Aid from the Research Committee of Surveillance and Infection Control of Prion Disease and from the Research Committee of Prion Disease and Slow Virus Infection, the Ministry of Health, Labour and Welfare of Japan.

Competing interests None.

Patient consent Obtained.

Ethics approval This study was approved by the Medical Ethics Committee of Kanazawa University and the Ethics Committees of the Tokushima University Hospital and Tokyo Medical and Dental University.

Contributors KF, MH, MS, TY, KSak, TH, NS, YS, KSat, SS, MY and HM: design/conceptualisation of the study. MH, KSak, TH, NS, YS, KSat, RA, KN, TM, SM and YI: acquisition of data. KF, MH, MS, RA, RK, MY and HM: analysis/interpretation of the data. MH: statistical analyses. KF, MH, MS, TY, KSak, TH, NS, YS, KSat, RA, SS, KN, TM, SM, YI, RK, MY and HM: drafting/revising the manuscript. All authors contributed to final approval of the version to be published.

Provenance and peer review Not commissioned; externally peer reviewed.

Data sharing statement There are no additional data available.

REFERENCES

1. Shiga Y, Miyazawa K, Sato S, *et al.* Diffusion-weighted MRI abnormalities as an early diagnostic marker for Creutzfeldt–Jakob disease. *Neurology* 2004;63:443–9.
2. Satoh K, Nakaoke R, Nishiura Y, *et al.* Early detection of sporadic CJD by diffusion-weighted MRI before the onset of symptoms. *J Neurol Neurosurg Psychiatry* 2011;82:942–3.
3. Chitravas N, Jung RS, Kofskey DM, *et al.* Treatable neurological disorders misdiagnosed as Creutzfeldt–Jakob disease. *Ann Neurol* 2011;70:437–44.
4. Zerr I, Kallenberg K, Summers DM, *et al.* Updated clinical diagnostic criteria for sporadic Creutzfeldt–Jakob disease. *Brain* 2009;132:2659–68.
5. Vitali P, Maccagnano E, Caverzasi E, *et al.* Diffusion-weighted MRI hyperintensity patterns differentiate CJD from other rapid dementias. *Neurology* 2011;76:1711–19.
6. Sasaki M, Ida M, Yamada K, *et al.* Standardizing display conditions of diffusion-weighted images by using concurrent b0 images: a multivendor multi-institutional study. *Magn Reson Med Sci* 2007;6:133–7.
7. Hirai T, Sasaki M, Meada M, *et al*; Acute Stroke Imaging Standardization Group-Japan (ASIST-Japan). Diffusion-weighted imaging in ischemic stroke: effect of display method on observers' diagnostic performance. *Acad Radiol* 2009;16:305–12.
8. Nozaki I, Hamaguchi T, Sanjo N, *et al.* Prospective 10-year surveillance of human prion diseases in Japan. *Brain* 2010;133:3043–57.
9. Masters CL, Harris JO, Gajdusek DC, *et al.* Creutzfeldt–Jakob disease: patterns of worldwide occurrence and the significance of familial and sporadic clustering. *Ann Neurol* 1979;5:177–88.